

## A Numerical Study of the Effect of the Mountainous Terrain of Japan on Tropical Cyclones

By Morris A. Bender and Yoshio Kurihara

*Geophysical Fluid Dynamics Laboratory/NOAA, Princeton University, P.O. Box 308  
Princeton, New Jersey 08542, U.S.A.*

*(Manuscript received 4 November 1986, in revised form 2 February 1987)*

### Abstract

A triply-nested, movable mesh model was used to study the effects of mountainous terrain on the landfall of tropical cyclones onto the islands of Japan. The integration domain spanned  $43^\circ$  latitude and  $47^\circ$  longitude with finest resolution of  $1/6^\circ$ . Numerical experiments were separately performed for three cases. In each experiment a storm was embedded onto a stationary Haurwitz type wave at the initial time, and moved in a north-northeast direction at about  $10$  to  $12 \text{ m s}^{-1}$ . In the first experiment, the tropical cyclone struck the southwest Izu Peninsula in eastern Japan. The second and third respectively made landfall on the Kii Peninsula in the central part of Japan and on the island of Kyushu in western Japan. In order to isolate some of the effects on the storm system resulting from its interaction with the mountainous terrain, these simulations were compared with supplemental experiments performed with a flat land condition. In all three cases it was found that the presence of the mountainous terrain greatly enhanced the storm decay after landfall. As the storm approached Tokyo Bay rapid weakening occurred as dry air from the mountain region to the west of Tokyo was advected into the eye and eyewall region of the storm. Upon leaving eastern Japan and again moving over open water, the storm never underwent reintensification. In the case of the storm leaving western Japan, reintensification over the Sea of Japan occurred very slowly as compared with the experiment run with a flat land distribution. Apparently, the above behavior was related to the structural change which occurred to the storm system during the passage over the mountainous islands. The precipitation pattern was also greatly affected by the presence of the mountainous terrain. As the storm made landfall over central Japan, the area of heaviest rainfall shifted to the right of the storm track, where strong upslope winds developed. This storm eventually travelled over the high mountains of east-central Japan and rapidly decayed by the end of the experiment.

Although performed for an idealized experimental design, these experiments reveal some of the important effects the mountainous terrain may have on the behavior of tropical cyclones making landfall on Japan. Understanding these effects should prove useful in forecasting more accurately the behavior of the storms.

### 1. Introduction

The behavior of a tropical cyclone is influenced by mountainous island terrain when it passes by or makes landfall onto the islands. Bender, Tuleya and Kurihara (1987, hereafter referred to as BTK) performed a numerical study to investigate the effects on a tropical cyclone due to the mountains of

the Greater Antilles in the northern Caribbean; Taiwan; and Luzon in the northern Philippines. These regions are all in the tropics and subtropics, where tropical cyclones generally move westward. In their triply-nested movable mesh model, realistic distributions of island topography were resolved at  $1/6^\circ$  resolution as the tropical cyclone approached the islands. It was found that the mountain-

ous islands modified the flow field, including both the basic flow and the winds associated with the vortex, causing displacement of the storm position as compared with the ocean only control case. Second, they found that the mountainous terrain could alter the structure of the tropical cyclones, making accurate determination of the storm position sometimes almost impossible. It was also concluded that the storm intensity was influenced through the moisture budget, as dry air was advected from the mountainous areas down to the storm and its surrounding environment.

In this paper, we will study the case of tropical cyclones encountering Japan. Each year, about ten tropical cyclones either move by or make landfall onto the Japanese Islands which are extremely mountainous in many places. In contrast to the cases treated in BTK, the islands of Japan lie in the middle latitudes and the approach of the storms to the islands are generally from the south or southwest. Accordingly, a moving tropical cyclone experiences an increase of the Coriolis parameter as it moves north.

It should be noted that, besides the presence of mountainous topography, a strong upper level westerly flow and sea surface temperature variation are other important factors which control the behavior of an actual tropical cyclone approaching Japan. However, in an attempt to isolate the mountain effects, we again perform the simulation experiments for a highly idealized condition similar to that used in BTK. Specifically, the basic flow we specify at the initial time does not have vertical shear and the sea surface temperature is fixed to a constant value.

In Section 2, the experimental design is briefly described. In the following sections, results will be shown for three sets of experiments in which a model typhoon made landfall onto eastern, central, and western Japan, separately. Some features of interest for each of the above cases are analyzed and the results are presented in Sections 3, 4, and 5, respectively, with a summary and concluding remarks presented in Section 6.

## 2. Experimental design

### a. Brief model description

The triply-nested, movable grid system originally described by Kurihara and Bender (1980) was used again for this study, with some specific model details outlined by Tuleya, Bender and Kurihara (1984). The model is an eleven level primitive equation model formulated in latitude, longitude and sigma ( $\sigma$ ) coordinates, with the outermost domain spanning 43° latitude (8.5-51.5°N) and 47° longitude (111.5-158.5°E). The model physics include cumulus parameterization described by Kurihara (1973) with some modifications (Kurihara and Bender, 1980, Appendix C), a Monin-Obukhov formulation for the surface flux calculation, and the Mellor and Yamada (1974) scheme (level 2) for the vertical diffusion. Similar to BTK, the surface temperature over water was set equal to 302K with the land surface temperature (LST) at each point determined by the following:

$$LST = 298 - \gamma_* z_* \quad (2.1)$$

Here  $\gamma_*$  was set equal to  $6.7 \text{ K km}^{-1}$ ,  $z_*$  being the surface height. Finally the roughness parameter was set to 25 cm at all land points.

### b. Topography description and integration procedure

Following BTK the distribution of  $z_*$  was first defined for the entire integration domain at the resolution of the finest mesh ( $1/6^\circ$ ). A particular grid point was considered to be a land point if the percent of water in a grid box was less than 81%. The values of  $z_*$  and percent water for the medium ( $1/3^\circ$ ) and coarse ( $1^\circ$ ) resolution were then determined by averaging the values of the fine resolution points that were covered by the area of each coarser mesh grid box. The distribution of  $z_*$  for each of the three grid resolutions is presented in Fig. 1, for part of the island of Japan.

A weak vortex, embedded in a Haurwitz type wave, was initially defined over an ocean environment, where it quickly intensified to typhoon strength. The wave was initially non-divergent and barotropic, with

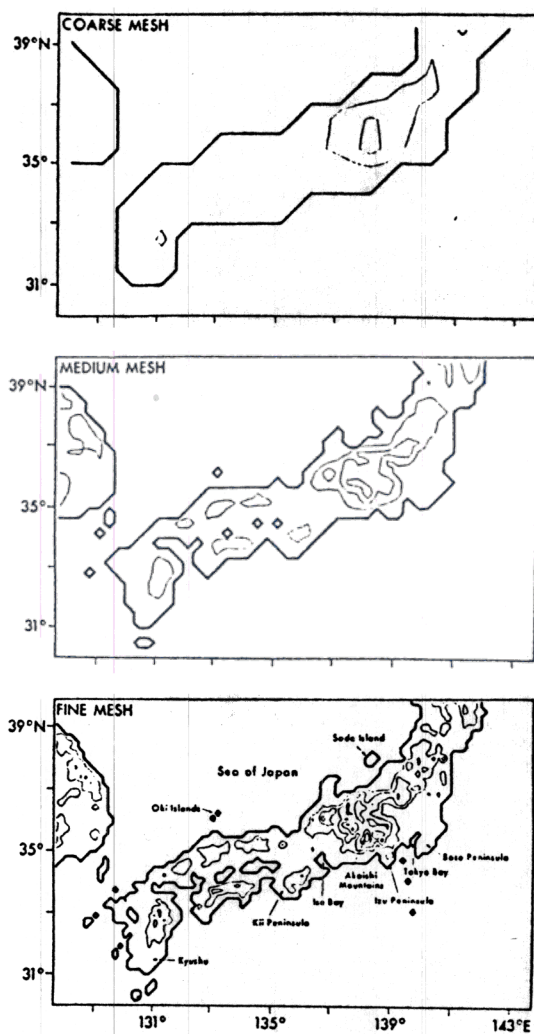


Fig. 1. The topographical distributions used for this study, at the coarse mesh ( $1^\circ$ ), medium mesh ( $1/3^\circ$ ), and fine mesh ( $1/6^\circ$ ) resolutions. The topographical heights are contoured at 500 m intervals.

the flow field derived at all levels from the streamfunction obtained by Phillips (1959):

$$\psi = -a^2 \omega \sin \phi + a^2 \kappa \cos^m \phi \sin \phi \cos m\lambda \quad (2.2)$$

Here,  $a$  is the radius of the earth,  $\lambda$  the longitude and  $\phi$  the latitude. The zonal wavenumber  $m$  was set equal to 8, with the constants  $\omega$  and  $\kappa$  set to  $1.657 \times 10^{-6} \text{ s}^{-1}$  and  $1.382 \times 10^{-6} \text{ s}^{-1}$  respectively. These selections made the wave barotropically stable and stationary. During the model initialization, the mass fields were obtained from the wind

field by solving a reverse balance equation.

At hour 39 for all the landfall simulations, when a vortex of typhoon strength was located at the axis of the wave trough, the land conditions and topography were inserted into the computational domain. In each experiment the computational domain was adjusted so that the storm moved toward the desired landfall position. During the integration, the values of  $z_*$  and LST at each grid point were kept in a data table for all three mesh resolutions. As the inner grids followed the storm and moved over the island topography, values of  $z_*$  and LST which were covered by the coarse resolution were replaced by their corresponding fine mesh values. See BTK for more information on the treatment of topography especially as the resolution changed.

### c. Summary of experiments

Three landfall simulations using the present distribution of topography were separately performed, with their storm tracks shown in Fig. 2. Landfall was made on the Izu Peninsula in eastern Japan (Exp. JE), the Kii Peninsula in central Japan (Exp. JC) and the island of Kyushu in western Japan (Exp. JW), respectively. Throughout the following sections results from these three integrations will be compared with an additional set of supplemental integrations (Exp. JEO, JCO and JWO) in which the typhoon made landfall at approximately the same three positions as the primary simulations. However, in these experiments the surface height ( $z_*$  over land was set to zero with a cool flat land surface condition ( $LST=298\text{K}$ ) at all points over the islands. The storm tracks for these experiments are shown in Fig. 3. These experiments helped to determine how much of the alteration of the storm structure during and after landfall was due to the effect of the land condition or the effect of the mountainous terrain itself. Comparisons will also be made with a control experiment: (dashed lines in Figs. 2 and 3) run with an identical initial vortex, but with ocean surface conditions at all grid points. In the ocean control experiment the storm tended

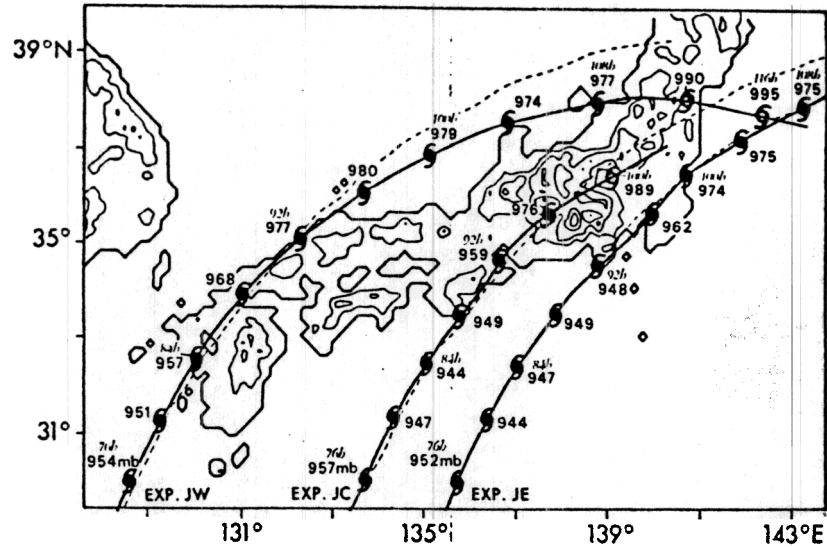


Fig. 2. Storm tracks for Exp. JE, Exp. JC and Exp. JW (thick solid lines) and the ocean only control case (dashed lines). The mountain heights are contoured at 500 m intervals, with the shoreline indicated by a thick solid line. Storm positions defined by the sea level pressure field, are plotted every 4 hours and indicated by a tropical cyclone symbol, with the storm's minimum sea level pressure (mb) indicated.

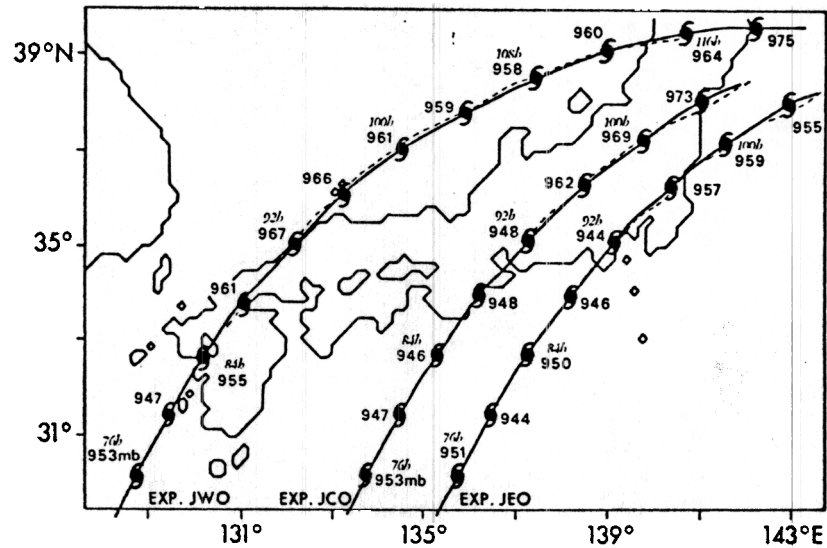


Fig. 3. Same as Fig. 2 but for Exp. JEO, Exp. JCO and Exp. JWO, run with the surface height ( $z_s$ ) equal to zero at all land points (flat land condition).

to be steered by the basic flow, although the actual storm track shifted slightly left (or to the north) of the initial stream function due to the beta effect. Some of the interesting features relating to the storm tracks of the six landfall experiments will be discussed in

the following three sections.

### 3. Eastern Japan

In this section results of the first pair of experiments (*i.e.* Exp. JE and Exp. JEO) will be discussed. The two storms made landfall

at approximately the same position on the southwest Izu Peninsula (Figs. 2 and 3). Fig. 4 indicates that the storms did not weaken before landfall. However, the storm in Exp. JE exhibited a small deceleration in its forward speed south of the island, landfalling at about 92 h, two hours after the storm in Exp. JEO. The translational speeds at landfall for the storms in Exp. JE and Exp. JEO were  $10 \text{ ms}^{-1}$  and  $11.2 \text{ ms}^{-1}$  respectively. In the eight hour period after landfall the minimum sea level pressure for Exp. JE and Exp. JEO rose 25.3 and 11.3 mb respectively, with the maximum low level ( $\sigma = .992$ ) winds decreasing by 16.1 and  $9.5 \text{ ms}^{-1}$  (Fig. 4).

While over open sea, the storm's horizontal scale before landfall, measured by the distance of the maximum low level wind location from the circulation center, was very similar for both Exp. JE and Exp. JEO as well as the experiments described later. The mean distance between the circulation center and

the location of the maximum low level wind was larger on the east and south side of the storms (about 45 and 46 km) than to the west and north (about 35 and 40 km). However, the distribution of this quantity fluctuated with time. Its azimuthal mean averaged

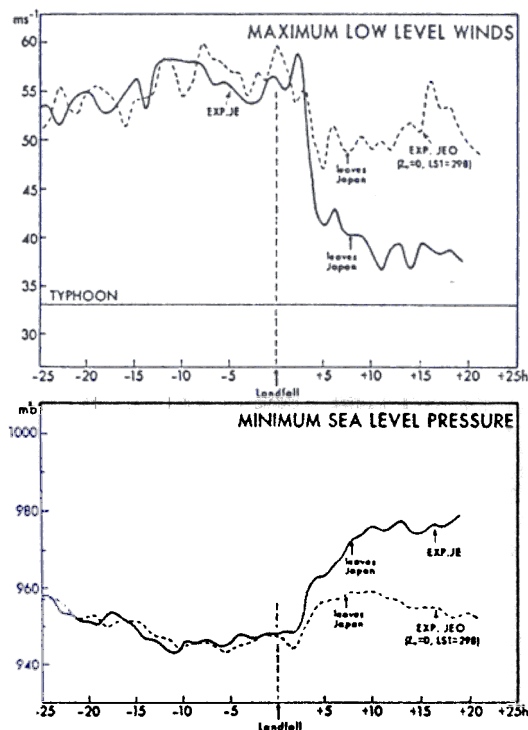


Fig. 4. Time series of maximum low level ( $\sigma = .992$ ) wind ( $\text{m s}^{-1}$ ) and minimum sea level pressure (mb) for the storms in Exp. JE (solid line) and JEO (dashed line). The time series are plotted relative to the time of landfall.

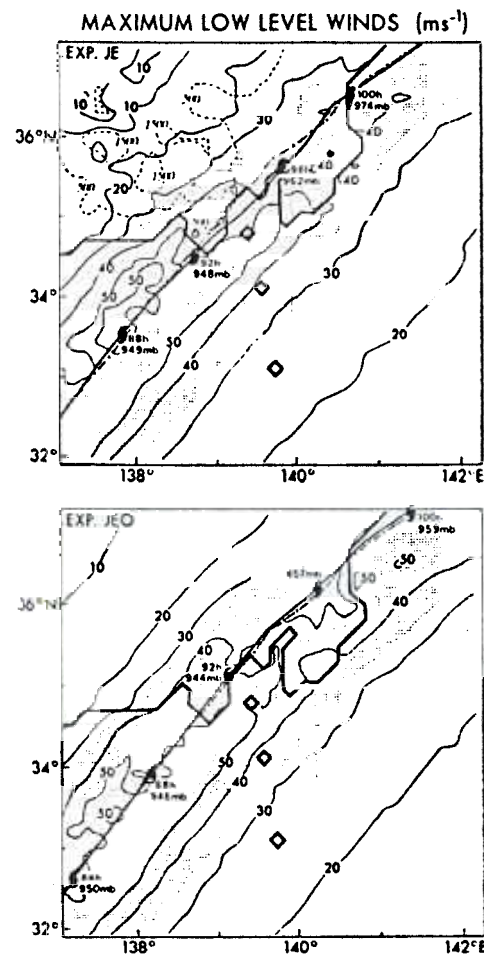


Fig. 5. Distribution of maximum low-level ( $\sigma = .992$ ) wind ( $\text{m s}^{-1}$ ) obtained at each grid point during the passage of the tropical cyclone for Exp. JE (upper) and Exp. JEO (bottom). The shading indicates wind speeds greater than typhoon force ( $33 \text{ m s}^{-1}$ ). The shoreline is indicated by a thick solid line with the 500 and 1500 m topographical height contoured (dashed line). The storm tracks are shown for each experiment, with the storm track for the ocean only control indicated by a thin dashed-dotted line. The storm positions at four hour intervals are indicated by a tropical cyclone symbol, with the minimum sea level pressure (mb) shown.

about 42 km for all the storms.

As the storm in Exp. JE made landfall, very heavy rainfall occurred in the region of very strong upslope on the eastern side of the Izu Peninsula. For example, a maximum rainfall of over 18 cm fell in the two hour period after landfall with a total of 28.3 cm falling at one location during passage of the storm.

After crossing the Izu Peninsula, the storm in Exp. JE was deflected about 30 km to the east of the ocean control case (Fig 5), moving over Tokyo Bay by 95 h. Although this deflection was small, it caused the storm's strongest winds to be confined east of Tokyo, in contrast to Exp. JEO, in which maximum winds greater than  $40 \text{ ms}^{-1}$  spread to the region to the west of Tokyo Bay. Also, we see from Fig. 5 that in Exp. JE the area of  $40 \text{ ms}^{-1}$  maximum winds did not reach to the northern end of Tokyo Bay, as the storm was beginning to rapidly weaken after 94 h.

An abrupt decrease of the maximum low level wind speed was observed at the coast in Fig. 5 for both Exps. JE and JEO. In particular some of the highest winds in Exp. JE during the period that the storm was over the land were located 65 km southeast of the storm center, just offshore of the Boso Peninsula. As the storms approached to the east coast, high winds greater than  $40 \text{ ms}^{-1}$  (Exp. JE) and  $50 \text{ ms}^{-1}$  (Exp. JEO) began to occur offshore.

Although the storm did not directly cross the mountainous terrain, we find from Fig. 6 (bottom) that dry air originating from the mountains in east-central Japan reached the eyewall region by 95 hours, when the storm was rapidly weakening. Actually, drier air was advected toward the storm region even before landfall (Fig. 6, top). However it appears the effect on the decay was small until the dry air began to encircle the eyewall at 94 h. This result agreed well with those obtained in BTK (*e.g.*, Fig. 12).

When the storm in Exp. JE approached the east coast of Japan at 99 h, a warm and dry region was formed about 40 km south of the storm center, in the layer between 3 and 7 km. Analysis indicated this phenomenon

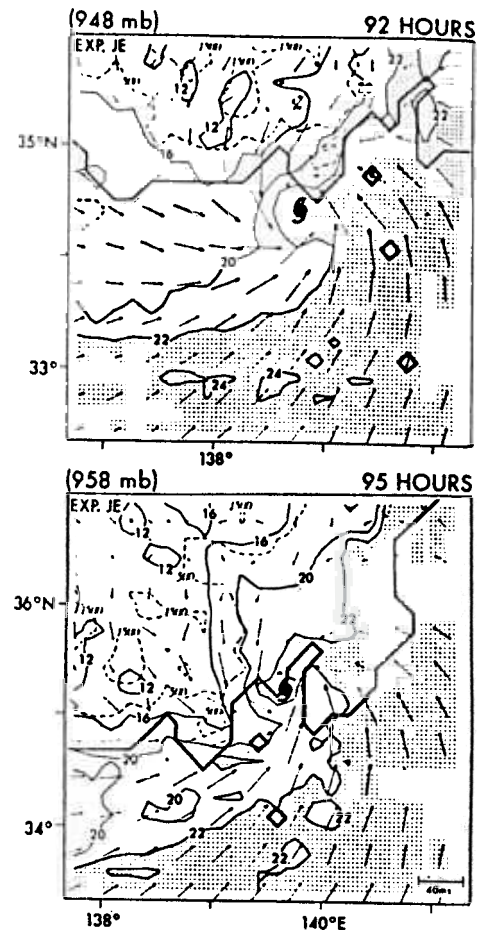


Fig. 6. Distribution of the horizontal wind vectors, mixing ratio fields (solid line) at model level 11 ( $\sigma = .992$ ) in the finest mesh for Exp. JE at 92 and 95 h. The shoreline is indicated by a thick solid line with the 500 m and 1500 m topographical height contoured (dashed line). Wind vectors are plotted at every other grid point. The areas with mixing ratio greater than  $22 \text{ g kg}^{-1}$  are shaded. The storm center, defined by the sea level pressure field, is indicated by a tropical cyclone symbol. The storm's minimum sea level pressure at each time level is given at the upper left of each frame.

was induced by subsidence as the storm circulation interacted with the mountainous topography. When the storm moved over the ocean, the maximum temperatures in the middle levels were found entirely within this region rather than below the storm's upper level warm core or above the surface center.

By 108 h this region was still located 50 km south-southeast of the storm center. This disorganization of the storm structure appears to have kept reintensification of the storm system from occurring during the final period of the integration (Fig. 4) although the storm was passing over a warm ocean environment once again. This result is somewhat similar to those obtained for Exps. L5 and L10 of BTK (*e.g.*, Fig. 20) where reintensification of the storm system west of Luzon was retarded until the entire storm system (*i.e.*, upper and lower mass and momentum fields) became vertically coupled again. In contrast, the storm in Exp. JEO remained vertically coherent during passage over Japan, and underwent slow reintensification beginning about two hours after leaving the east coast of Japan.

#### 4. Central Japan

In this section results of Exps. JC and JCO will be discussed. From Figs. 2 and 3 we see that landfall for the two storms occurred at approximately the same location on the coast of the southern Kii Peninsula. Similar to Exp. JE, the translational speed of the storm in Exp. JC decreased south of Japan, as compared with Exp. JCO and the ocean control, and the storm made landfall about 1.5 hours later (88 h). The translational speeds at landfall for the storms in Exps. JC and JCO were about  $9.9 \text{ ms}^{-1}$  and  $10.8 \text{ ms}^{-1}$  respectively. From Fig. 7 we again see that little storm decay occurred before landfall. This is similar to the reduced storm decay of the simulations in BTK performed with the faster  $10 \text{ ms}^{-1}$  basic flow. This agrees with our speculation that storm decay before landfall onto mountainous islands may often be reduced when the storm is embedded in a strong basic flow and is moving with a fast translational speed (see Table 3 of BTK). For the first 5 hours after landfall, the storm decay in Exp. JCO was small, as the storm paralleled the coast. In contrast, the storm in Exp. JC immediately began to weaken after landfall, as the storm center moved over the coastal mountain ranges and very dry air was advected into

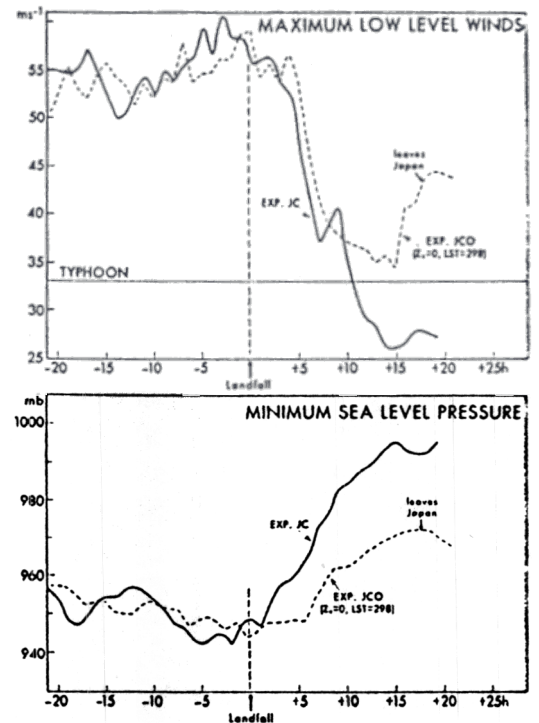


Fig. 7. Same as Fig. 4 but for Exp. JC (solid line) and Exp. JCO (dashed line).

the storm circulation. In the first eight hours after landfall, the minimum sea level pressure rose 27.5 mb (Fig. 7) in Exp. JC, with a 17 mb filling for Exp. JCO.

As the storm moved further inland and its circulation began to interact with the mountainous terrain northeast of the storm, a secondary region of strong winds developed near and slightly southwest of the highest peaks of the southern Akaishi Mountains (2000 m contour in the model topography). At 95 hours (about 7 hours after landfall) the storm's maximum winds were located just to the southwest of the above mentioned 2000 m height contour, about 90 km east of the storm center. This type of interaction resulted in a spike in the time series of maximum low level winds between 7 and 10 hours (Fig. 7), observed after landfall in Exp. JC. Hence, the maximum low level ( $\sigma = .992$ ) wind during the first eight hours after landfall decreased only by  $16.1 \text{ ms}^{-1}$  in Exp. JC compared to  $18.9 \text{ ms}^{-1}$  for Exp. JCO. A similar feature was observed in

Exp. M (*i.e.* Fig. 4) of Bender, *et al.* (1985) as the model tropical cyclone crossed the mountain peak of their idealized mountain range.

As the storm passed the Ise Bay it was deflected about 20 km to the west of the track of the ocean control, similar to the eastward deflection of Exp. JE. These small deflections may have resulted from the flow field tending to curve around the high mountain block. As the storm in Exp. JC continued to move inland over the mountainous region in east central Japan, rapid weakening continued, with the entire storm becoming very disorganized by the end of the simulation. In contrast, the filling rate of the minimum sea level pressure for the storm in Exp. JCO leveled off as the storm approached the eastern coast, with reintensification beginning two hours after the storm center once again moved over the open waters.

The topography also greatly affected the storm rainfall distribution (Fig. 8). For both Exp. JCO and the ocean control, the largest total rainfall was observed primarily to the left of the storm track for most of the simulation, as the convective cells in the eyewall region rotated cyclonically around the moving storm center. However, after 92 h the area of largest storm rainfall tended to shift to the right of the storm track in Exp. JC, *i.e.*, toward the region of strong upslope wind. Likewise, the region of downslope to the left of the storm track was marked by a noticeable decrease in rainfall. Thus, northeast of the storm position at 94 hours, the 10 cm rain contour line in Fig. 8 (top) shifted to the right of the track. Also, an enhanced area of very large total rainfall (*e.g.* greater than 15 cm) was located almost entirely to the right of the storm track, from just east of Ise Bay to the Akaishi Mountain Range. Another effect of the topography was an increase in the area over Japan which received light rainfall. This region was bounded by the 1 cm contour at the top of Fig. 8.

##### 5. Western Japan

In this section results of Exp. JW<sub>2</sub> and

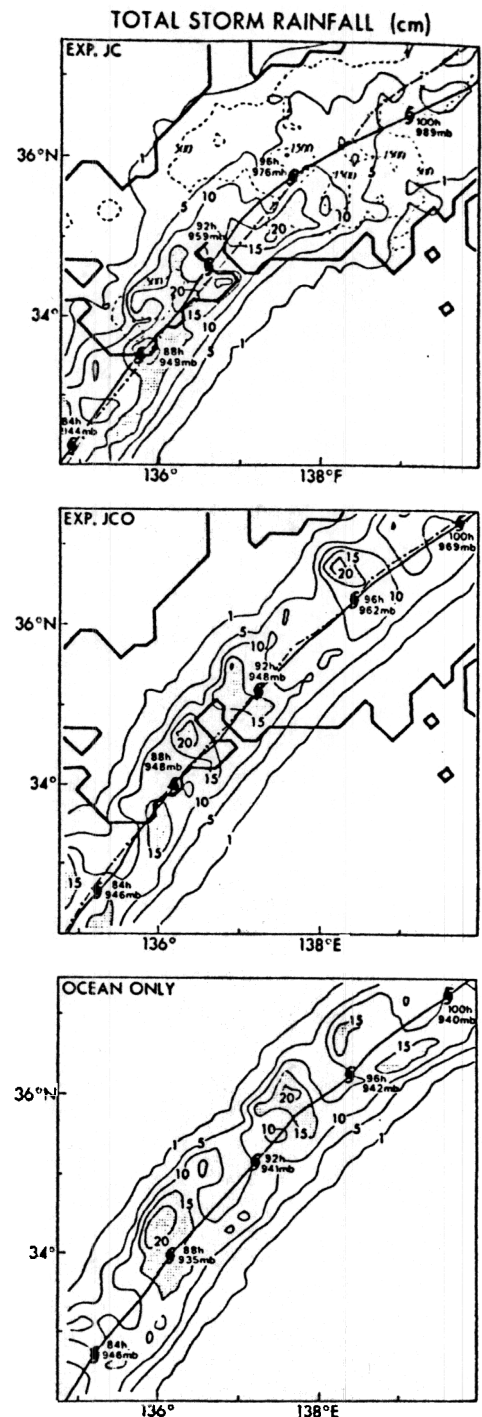


Fig. 8. Distribution of the storm total rainfall (cm) obtained at each grid point during the passage of the tropical cyclone for Exp. JC (upper figure), Exp. JCO (middle figure) and the ocean only control (bottom figure). Total rainfall greater than 15 cm is shaded. See Fig. 5 for more details.

JWO will be discussed and compared with each other. From Figs. 2 and 3 we see that landfall for both typhoons again occurred at approximately the same location onto western Kyushu, at about 84 and 83 hours, with a minimum sea level pressure and translational speed for the two experiments at landfall of 957 mb and  $11.4 \text{ ms}^{-1}$  and 954 mb and  $10.9 \text{ ms}^{-1}$  respectively. In both experiments rapid weakening began about three hours before landfall, as the storm moved parallel to the west coast of Kyushu and passed near the Koshikijima island lying off the coast. During this time the storm's low level winds, particularly over the islands, were reduced by the enhanced surface friction. The resulting distortion in the wind field possibly contributed to the storm weakening before the storm center finally moved onto Kyushu. The minimum sea level pressure fell about 21 mb and 14 mb respectively for the two experiment (Fig. 9) during the approximately eight hour period in which the storms were

over land. During this same period the maximum low level winds ( $\sigma = .992$ ) decreased by  $15.8 \text{ ms}^{-1}$  in Exp. JW and  $6.2 \text{ ms}^{-1}$  in Exp. JWO.

While the storms in both Exps. JW and JWO were well south of the west coast of Kyushu, a distinct rain free region (the eye) was observed near the position of the surface pressure minimum. However as the storm approached the coast (about 2 hours before landfall) the eye position in Exp. JW became slightly displaced from the surface pressure minimum and the circulation centers. By the time of landfall at 84 hours, the eye was located 35 km southwest of the surface pressure minimum, finally crossing the coast at 85 hours. At this time the eye was about 40 km to the southwest of the pressure minimum. As the storm continued to move inland, the eye remained displaced well to the southwest, until becoming obscured by light rain by 87 hours. (A similar tendency for displacement of the eye from the pressure center at landfall occurred in Exp. JE.). During this period after landfall, the area of heaviest rainfall intensity in Exp. JW tended to be located entirely to the east of the pressure minimum. Analysis of the boundary layer convergence field indicated that the area of strongest convergence existed primarily to the right of the storm during this time. No distinct rain free area was again observed near the storm center even after 94 hours when the storm was again over the Sea of Japan.

Although the eye in Exp. JWO crossed the west coast of Kyushu with very little displacement from the surface pressure minimum, we see (Fig. 10) that significant changes in the eye structure occurred soon after landfall, even without the presence of topography. During this time, the eye gradually became obscured, as the area of boundary layer moisture divergence (unshaded area of Fig. 10) near the center of the storm also weakened, almost disappearing by 87 hours. This indicates that changes in the surface condition had a significant influence on the eye dynamics of the storm. Indeed, cross sections through the storm region indicate

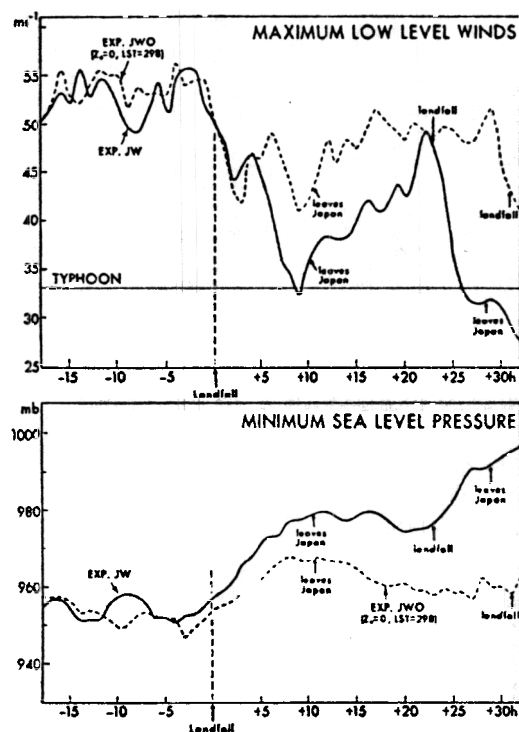


Fig. 9. Same as Fig. 4 but for Exp. JW (solid line) and Exp. JWO (dashed line). The time series are plotted relative to the time of the first landfall.

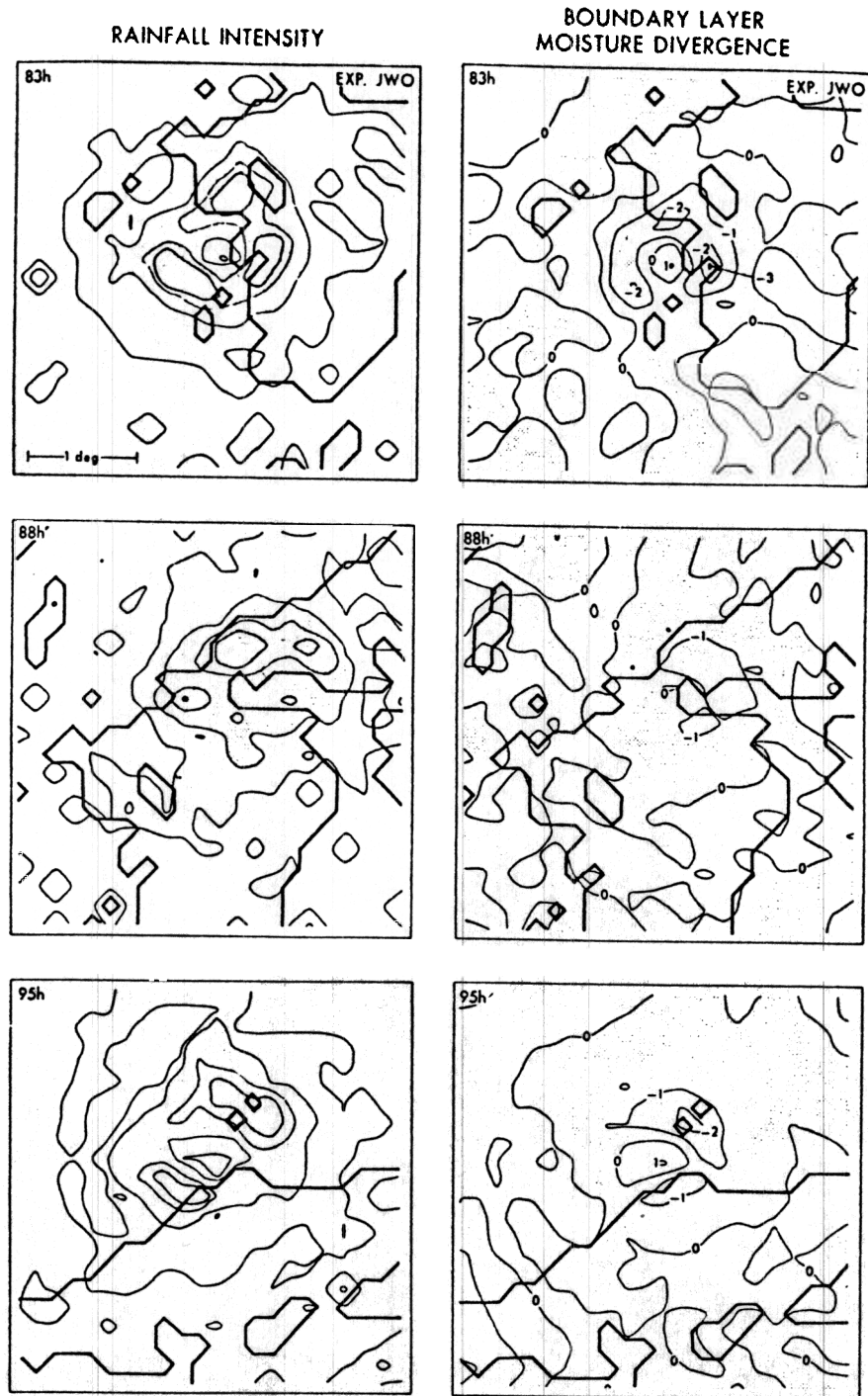


Fig. 10. Rainfall intensity (left,  $\text{cm h}^{-1}$ ) and boundary layer moisture divergence (right,  $10^{-3} \text{ gm cm}^{-2} \text{ sec}^{-1}$ ) in the finest mesh area for Exp. JWO at 83, 88, and 95 h. The latter quantity is calculated by vertically integrating the moisture divergence from the surface to  $\sigma = .86$ , with areas with negative values (convergence) shaded. Rainfall intensity between  $.5 \text{ cm h}^{-1}$  and  $2.5 \text{ cm h}^{-1}$  is lightly shaded with values greater than  $2.5 \text{ cm h}^{-1}$  having thicker shading and an additional contour of  $5 \text{ cm h}^{-1}$  drawn within the thicker shading. Finally, rainfall intensity of  $.05 \text{ cm h}^{-1}$  is also contoured.

that the vertical structure of the eye and eyewall region throughout much of the atmosphere was altered soon after landfall. During this period there was also some tendency for the region of strongest moisture convergence (and heaviest rainfall) to become displaced to the east of the storm position. However, as the eyewall region approached the Sea of Japan, the region of boundary layer moisture divergence began to grow in size once again with the eye (rain free area) reappearing by 91 hours at a position near the north coast of the island. During the next several hours the eye moved northeast along the coast, until emerging over the open water by 95 hours. As expected, the regions of strong boundary layer moisture convergence were well correlated with the regions of strongest convection.

By 96 h (twelve hours after landfall) the storms in both Exps. JW and JWO were over the Sea of Japan east of the Oki islands. Similar to the storm in Exp. JE, analysis indicated that a distinct warm region in the middle levels formed southeast of the upper level (8.1 km) warm core and surface pressure center in Exp. JW. However, the mass field became vertically coherent again by 102 h, when deepening of the minimum sea level pressure once again commenced. In contrast, the entire storm system in Exp. JWO remained vertically coherent during passage over land, and deepening of the storm system began soon after the storm center moved over the warm ocean environment.

Another feature observed in Exp. JW was the noticeable acceleration in the storm's translational speed after it entered the Sea of Japan (Fig. 2) with the storm track deflecting to the right of the storm track of both the ocean only control experiment and Exp. JWO. In Exp. JW the storm made a second landfall onto the northwest coast of Japan about 23 hours after the first landfall, rapidly decaying to tropical storm strength and filling over 18 mb in the next 8 hours. Upon leaving the east coast of Japan and travelling over the open waters once again, the storm continued weakening, with a minimum sea level pressure of 996 mb by the

end of the experiment. In Exp. JWO the storm made a second landfall 31 hours after the first landfall, weakening 15 mb in the next eight hours.

## 6. Summary and concluding remarks

The effects of Japan's mountainous terrain on tropical cyclones were simulated for typhoons making landfall onto eastern, central and western Japan. When comparison was made with the landfall simulations run with flat land conditions everywhere, it was found that the mountainous terrain greatly enhanced the decay rate of the storms, even when the storm track did not directly cross the mountainous region. During the eight hour period following landfall, the filling rate of the minimum sea level pressure compared with each of the flat land simulations increased from 11.3 to 25.3 mb, 17 to 27.5 mb, and 14 to 21 mb for the three sets of experiments. During the same eight hour period, the filling rates of the storms in Exps. T10, L10 and C10 of BTK were 24 mb, 23 mb, and 16 mb respectively. Similar to BTK, one of the chief causes of the enhanced decay was the advection of dry air from the mountainous regions into the storm circulation. For the case of eastern Japan, the source region of the dry air was located well west of the storm track. The storms exhibited little decay prior to landfall except for Exps. JW and JWO, which began weakening about three hours before landfall. These results are in good agreement with the faster moving storms of BTK. We believe that the storm's translational speed (or magnitude of the basic flow) is an important factor for influencing the storm decay rate before landfall onto mountainous terrain.

In the case of Exp. JE the mountainous terrain also deflected the storm about 30 km further to the east of the storm of Exp. JEO and the ocean control. This resulted in the storm crossing the center of Tokyo Bay, with the strongest winds occurring east of Tokyo. Likewise the storms in Exp. JC and JW were deflected after landfall about 20 km to the west of the track of the ocean control. This deflection may have resulted from a small

tendency of the flow field to curve around the mountain block. The most significant track deflection observed, along with accelerated movement, occurred in Exp. JW where the storm track gradually shifted to the right of the track of the ocean control and Exp. JWO, after the storm entered the Sea of Japan. It is uncertain whether these track deviations and speed changes were primarily due to interaction of the storm system with the topography or due to interactions between the large scale Haurwitz wave and the topography. Otherwise, the mountain terrain did not appear to cause other significant track changes, especially compared to some of the track deflections observed in BTK. This suggests the large variability that these mountain effects may have with the different topographical distributions and flow fields being considered.

The distribution of the maximum wind showed an abrupt decrease in its magnitude at the coast. After landfall, some of the storm's strongest winds at various times were located a considerable distance from the storm center, either just offshore (Exp. JE) or near the high mountain peaks (Exp. JC).

Similar to BTK the mountainous terrain greatly affected the rainfall distribution as well. For example, after landfall over central Japan, the region of heaviest rainfall shifted entirely to the right of the track where the storm's winds ascended the mountainous terrain, with reduced rainfall in the down-slope regions to the left of the storm track. As the storm made landfall on the Izu Peninsula, a maximum rainfall of over 18 cm fell in a two hour period in the region of steep upslope on the eastern side of the peninsula.

After crossing Japan we found that the vertical structure of the storm was altered in both Exps. JE and JW. In Exp. JE an anomalously warm and dry region formed in the middle of the atmosphere, originally induced by subsidence as the storm was passing east of the mountainous terrain. This area remained displaced from the storm center and upper level warm core even after the storm system was again passing over

open waters. This apparently prevented reintensification of the storm system. For the storm in Exp. JW, some deepening of the system again commenced once the storm's vertical coherence was reestablished.

The results of the present experiments confirm many of the conclusions obtained in BTK concerning the behavior of tropical cyclones in regions of mountainous islands. This was true despite the differences between some of the experimental conditions of the present study and those of BTK. Although these experiments were performed for an idealized flow field and experimental design, it is believed that many of the important mountain effects were isolated, revealing some of the significant interactions between the topography and typhoons striking Japan. Hopefully these results will prove useful to forecasters, although verification of these results with observations has yet to be made. Nevertheless, these important effects cannot be ignored as we attempt to improve our understanding of the behavior of tropical cyclones making landfall in this region. Such effects should be included in a dynamical model for typhoon prediction.

#### Acknowledgements

The authors would like to thank J. Mahlman for his continuous support of the hurricane dynamics project of GFDL. They would like to express their appreciation to R. E. Tuleya and C. L. Kerr of GFDL, and H. Kida of the GFD Program of Princeton University for their valuable comments and criticisms on the original version of this manuscript. Credit is also given to P. Tunison, K. Raphael, J. Varanyak and J. Conner for preparing the figures.

#### References

- Bender, M. A., R. E. Tuleya and Y. Kurihara, 1985: A numerical study of the effect of a mountain range on a landfalling tropical cyclone. *Mon. Wea. Rev.*, **113**, 567-582.
- , ——— and ———, 1987: A numerical study of the effect of island terrain on tropical cyclones. To be published in *Mon. Wea. Rev.*, **115**, 130-155.

- Kurihara, Y., 1973: A scheme of moist convective adjustment. *Mon. Wea. Rev.*, 101, 547-553.
- and M. A. Bender, 1980: Use of a movable nested mesh model for tracking a small vortex. *Mon. Wea. Rev.*, 108, 1792-1809.
- Mellor, G. L. and T. Yamada, 1974: A hierarchy of turbulence closure models for planetary boundary layers. *J. Atmos. Sci.*, 31, 571-583.
- Phillips, N. A., 1959: Numerical integration of the primitive equations on the hemisphere. *Mon. Wea. Rev.*, 87, 333-345.
- Tuleya, R. E., M. A. Bender and Y. Kurihara, 1984: A simulation study of the landfall of tropical cyclones using a movable nested-mesh model. *Mon. Wea. Rev.*, 112, 124-136.